The Earth Radiation Budget Experiment (ERBE)

Bruce R. Barkstrom

Atmospheric Sciences Division
NASA/Langley Research Center
Hampton, VA 23665

Abstract

The Earth Radiation Budget Experiment (ERBE) is the first multi-satellite system designed to measure the Earth's radiation budget. It will fly on a low-inclination NASA satellite and two Sun-synchronous NOAA satellites during the mid-1980s. Each satellite will carry two instrument packages—a scanner and a nonscanner—each package containing a complete, traceable system for inflight calibration. The nonscanner package has four Earth-viewing channels, as well as a solar monitor similar to that flown on the Solar Max Mission. The nonscanner detectors are the first Earth-viewing active cavity radiometers. The scanner package contains three thermistor bolometers which scan the Earth perpendicular to the orbital track.

The data from the satellite radiometers will be brought to the top of the atmosphere using a pixel-by-pixel process for the scanner data and a numerical filter for the nonscanner. The inversion will use angular directional models based on the Nimbus 7 ERB instruments, selecting the appropriate model for cloud conditions from the ERBE scanner data. After the measurements have been brought to the top of the atmosphere, they will be averaged over time to produce monthly averages. In averaging, allowance will be made for meteorological variations, as well as albedo variations with solar zenith angle. These new features are expected to provide a substantial improvement in the accuracy of the radiation budget on regional as well as global scales. This paper also provides a brief description of the implementation of the ERBE Project, including the ERBE Science Team.

1. Introduction

Because of its scientific importance, the Earth's radiation budget will be measured by instrument packages flying on three satellites in the mid-1980s. This three-satellite mission, known as the Earth Radiation Budget Experiment (ERBE), is the result of the interest of the scientific community in providing a continuing record of radiation budget changes, as well as the desire to obtain more accurate measurements through improved sampling.

As has been known since the early decades of this century, the absorbed solar energy is approximately in balance with the energy emitted by the Earth and its atmosphere when considering time scales on the order of years (Vonder Haar and Suomi, 1969; Ellis *et al.*, 1978). Indeed, the study of possible changes in the energy balance of the Earth caused by changes in the flow of radiation is one of the cornerstones of modern climate modeling (Schneider and Dickinson, 1974; Ramanathan, 1977). On shorter time scales and over smaller regions than the entire globe, there are imbalances between the absorbed and emitted energies that drive both atmospheric and oceanic circulation systems (Lorenz, 1967; Oort and Vonder Haar, 1976). Due to the close ties between the energy sources and these circulations systems, measurements of the radiation budget provide one of the important tools for the validation of numerical models of the atmosphere (Hartmann and Short, 1980; Slingo, 1982). They also provide possibilities for "climate experiments" by allowing the sensitivity of the radiation budget to various forcings to be studied empirically (Cess, 1976; Ohring and Clapp, 1980; Cess *et al.*, 1982).

Initial steps towards ERBE were taken in 1975 with a workshop at the National Center for Atmospheric Research. The National Academy of Sciences reviewed the NASA radiation budget program and provided requirements for measurement accuracy and spatial and temporal coverage. NOAA, as well as various university and industry representatives, reviewed the scientific requirements and approach, and agreed to the instrument concept and satellite complement. In 1979, the Earth Radiation Budget Experiment was approved by the United States Congress as a NASA project. The objectives of the ERBE, which resulted from this lengthy process, are given in Table 1.

Attempts to measure the radiation budget of the Earth

TABLE 1. ERBE objectives and capabilities.

Measurement[a]	Required Accuracy ($W \cdot m^{-2}$)	ERBE Capability[b] ($W \cdot m^{-2}$)
Solar Constant	1.0 to 10.0	3.0
Reflected and Emitted Radiant Exitance		
Global Net	1	1.3
Equator-to-pole Gradient	4	2
Zonal, 10°	2-12	5
Regional, 2.5°	2-15	10

[a] Based on observing period of one month. [b] Estimated.

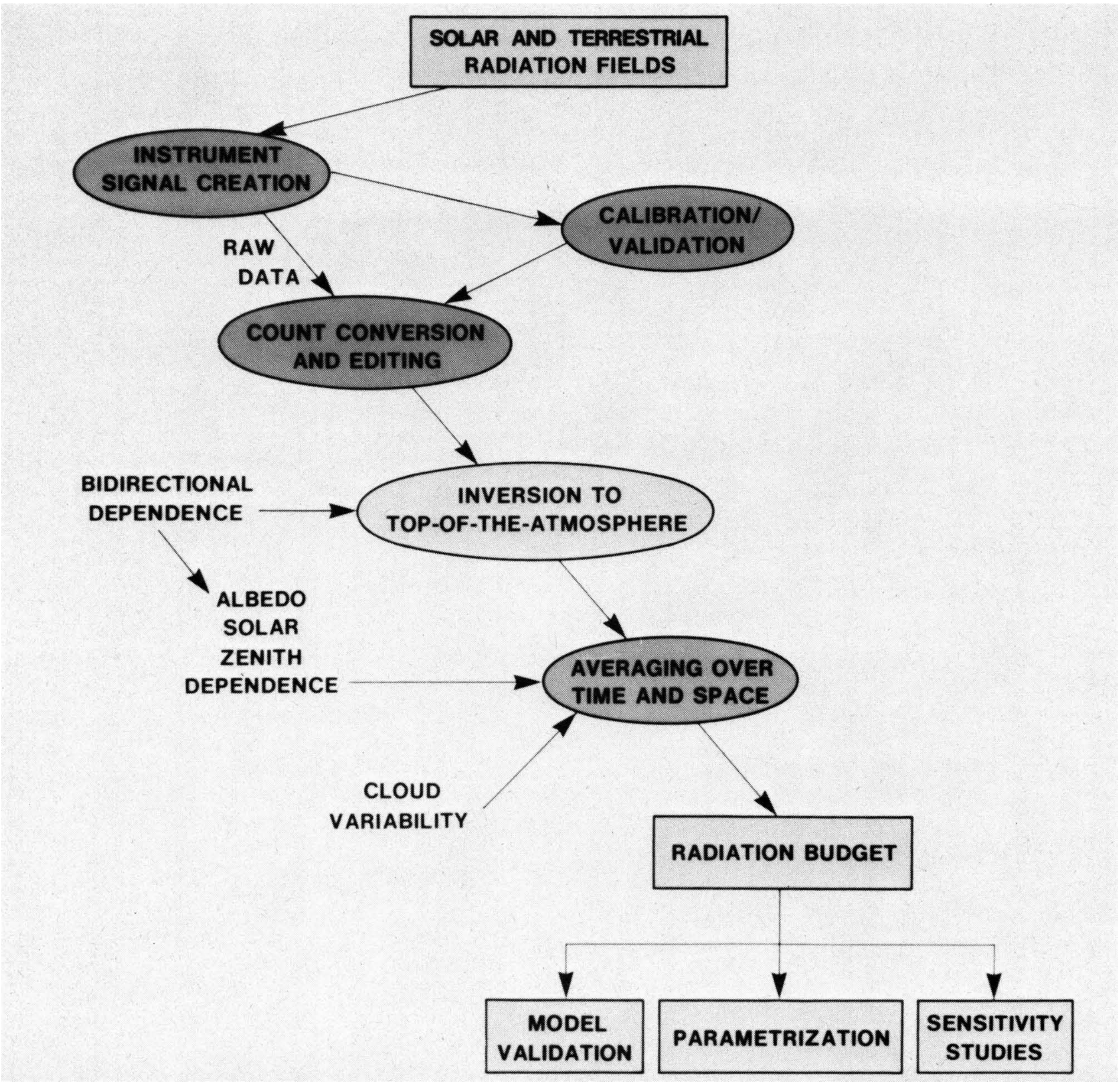

FIG. 1. Data flow diagram for Earth radiation budget data processing. Radiation reflected and emitted from the top of the atmosphere goes through the processes shown in this figure to produce estimates of monthly, regional averages of the radiation budget. The radiant exitances are sampled and detected by the satellite radiometers, where they are converted to counts and transmitted to Earth. The ground-processing system must convert the counts to estimates of the radiation striking the instruments, invert the satellite altitude radiation fields to the top of the atmosphere, and average these fields over time and space.

have been made since the beginning of the satellite era (Suomi, 1958; Vonder Haar and Suomi, 1969; Vonder Haar, 1969 and 1970; Raschke *et al.*, 1973; Smith *et al.*, 1977; as well as the recent survey by Stephens *et al.*, 1981). Nonetheless, a satellite system to measure the radiation budget is not simple, as was noted by Bignell (1961). Any radiation budget measurement system contains not only the satellite radiometers, but also data-processing software. This combination must convert the satellite data into instantaneous estimates of the radiation striking the detectors, reduce the satellite altitude radiation fields to the top of the atmosphere, and finally average them over time and space, as shown in Fig. 1. Each step in the estimation process contains potential sources of uncertainty that should be minimized where possible. For the ERBE, the concentration on error reduction has led to the first Earth-viewing use of active-cavity radiometers, a complete onboard calibration system, and numerous improvements in the inversion and averaging algorithms. These will be described in the remainder of this paper, together with the implementation of the experiment.

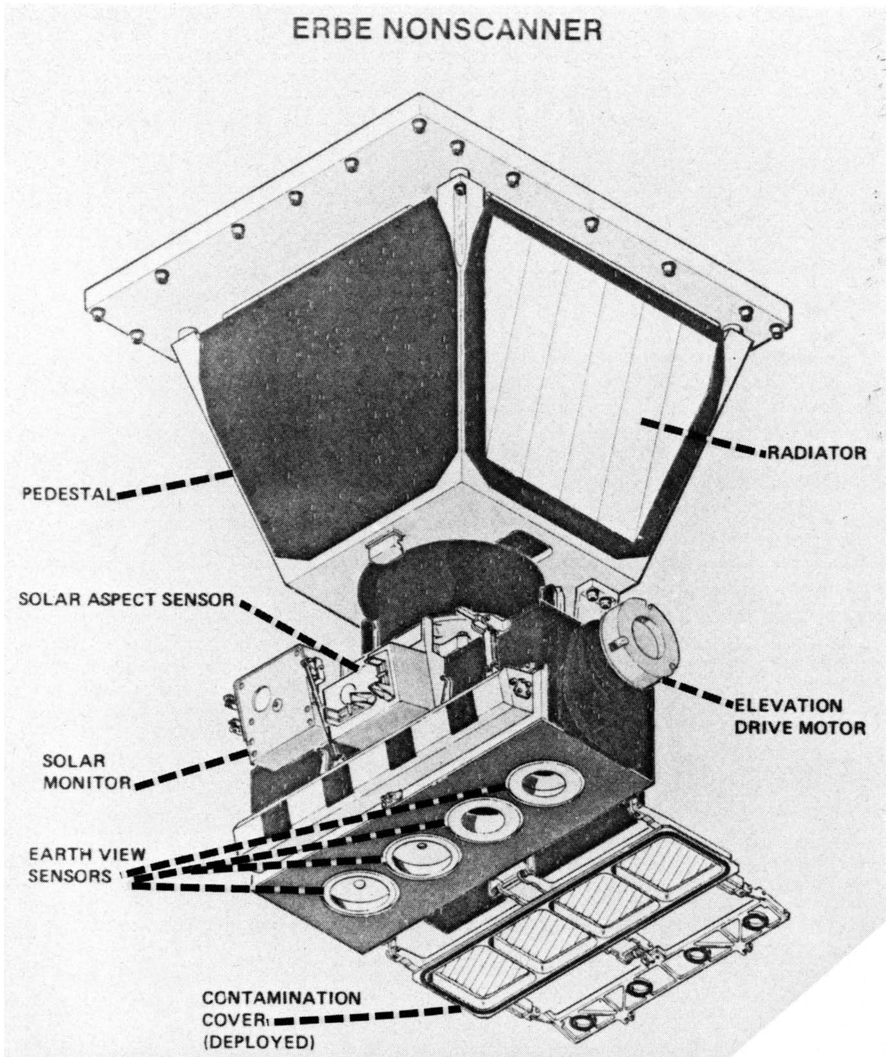

FIG. 2. ERBE nonscanner instrument package. The nonscanner instrument package has four Earth–viewing channels and a solar monitor. All five instruments are active cavity radiometers for spectral flatness and electrical substitution radiation detection. The Earth–viewing channels have two limb–to–limb (WFOV) channels, and two channels that have a ground footprint about 1000 km in diameter (MFOV channels). Each pair of channels has one total channel, and one channel to detect shortwave radiation.

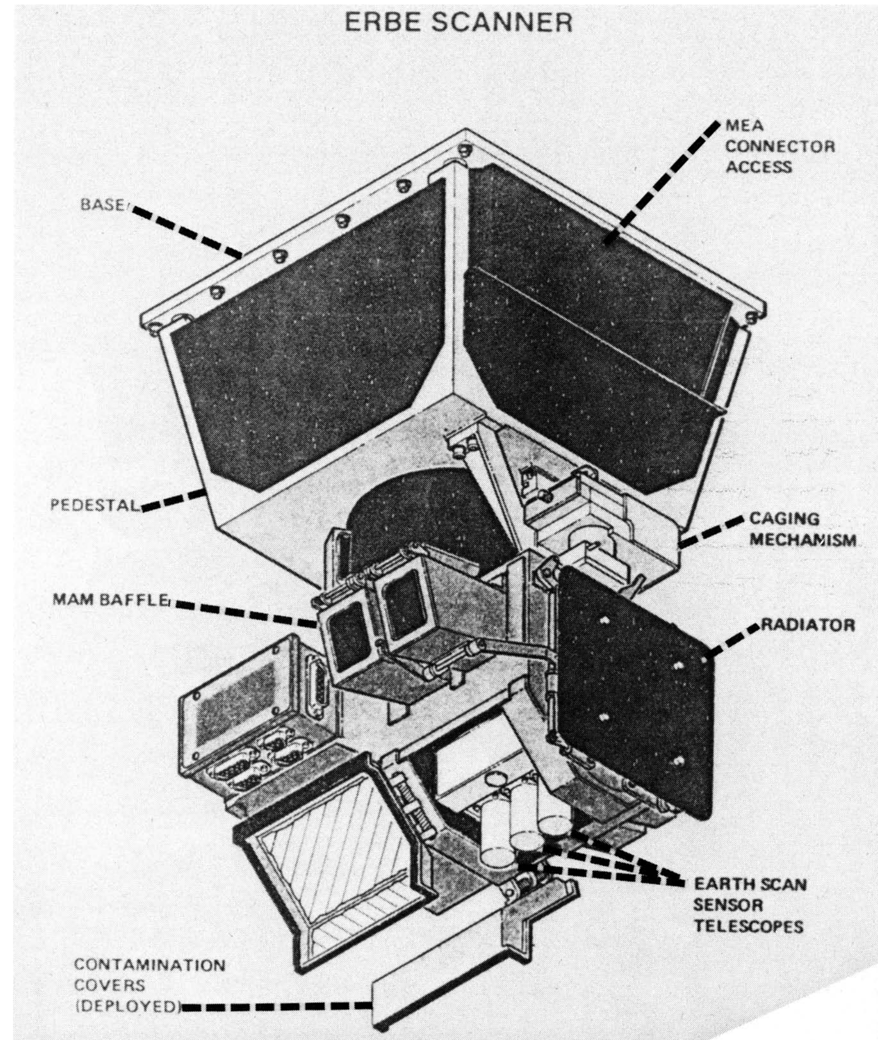

FIG. 3. ERBE scanner instrument package. The scanner instrument package has three Earth–viewing channels that normally scan crosstrack. The baffles for the mirror attenuator mosaic (MAM), which serves as a diffuser plate for solar calibration, are also visible. The three channels serve to detect all wavelengths, shortwave (0.2 to 5 μm) radiation, and longwave radiation (5 μm to 50 μm). Ground footprint at nadir is about 35 km crosstrack and 45 km along track.

TABLE 2. ERBE instrument parameters.

Platform	Package	Envelope (cm) Diameter	Height	Length	Width	Weight (kg)	Power (W)	Sampling rate (samples/s)
ERBS	Nonscanner	46	42	—	—	30	15	1.25
	Scanner	—	36	33	30	25	35	120
TIROS	Nonscanner	46	57	—	—	30	15	1.25
	Scanner	—	36	33	30	25	35	120

2. The instrument portion of the ERBE measurement system

On each of the three satellites that will carry the ERBE instruments, there will be two instrument packages, as shown in Figs. 2 and 3 and summarized in Table 2. One package contains four Earth-viewing detectors and a solar monitor. The other contains a scanner with three detectors to measure shortwave (0.2 to 5 μm), longwave (5 to 50 μm), and total waveband radiation (shortwave and longwave together). Both packages provide calibration traceability to the International Practical Temperature Scale—1968 (IPTS68) and to the solar constant. The ties to the IPTS68 are made with ground and inflight blackbodies that contain platinum resistance thermometers (PRTs). The ties to the solar constant are made by solar observations in special operating modes. In addition, detailed analytical models of the instruments' operation have been developed to provide ties between the underlying physics by which the radiation is detected and the equations used in data reduction. These models have provided important insights into the proper design choices for the instruments. The emphasis on being able to treat the ERBE instruments theoretically, as well as empirically, represents a significant advance in our ability to assess the accuracy and statistical significance of the final results.

a. The nonscanner instruments

Each nonscanner instrument package has four Earth-viewing channels and a solar monitor, as shown in Fig. 2. The Earth-viewing channels have two "spatial resolutions": a limb-to-limb view of the Earth, and a field of view limited to about 1000 km in diameter. The former are often called the wide field-of-view (WFOV) channels and the latter, medium field-of-view (MFOV) channels. For each of the two fields of view, there is a total spectral channel, which is sensitive to all wavelengths, and a shortwave channel, which uses a high-purity, fused silica filter dome to transmit only the radiation from 0.2 μm to about 5 μm.

Because of the concern for spectral flatness and high accuracy, all five of the channels on the nonscanner package are active-cavity radiometers. A shortwave detector is shown in Fig. 4. The radiation detected by each radiometer is absorbed on the inside surface of a black, specularly lacquered silver cone. Any light that is reflected after it first strikes the surface of the cone is reflected at least twice more, greatly limiting the energy that might emerge from the entrance aperture. Thus, the cavities are quite insensitive to spectral variations in lacquer reflectivity.

The cavities detect radiation by very accurately determining the electrical power required to keep the temperature of the cavity constant. The outside of each cone is wrapped with an electrical heater wire. As more radiation falls on the cavity, less electrical power must be dissipated in the heater wires to maintain a constant cone temperature. This electrical substitution principle is the most accurate broadband detection method available and is being used in all of the instruments making up the World Radiometer Reference (WRR) as well as the Solar Max ACRIM instruments (Willson *et al.*, 1981).

The ERBE solar monitor is a direct descendent of the Solar Maximum Mission's (SMM) ACRIM detector. The ERBE instrument differs from the ACRIM design primarily in three areas: a slightly smaller heat sink, a slightly faster electronics, and a considerably larger field of view. The latter difference arises because the ERBE monitor is designed to operate with the Sun drifting through the field of view, while the SMM/ACRIM instrument was designed to be continuously pointed by the spacecraft. It is expected that ERBE and SMM/ACRIM will have similar capabilities.

Thermally operated instruments are potentially sensitive to extraneous heat flows. Therefore, great care has been exercised in dealing with the heat flow within the instruments. The cavities are enclosed in a module that is mounted in a

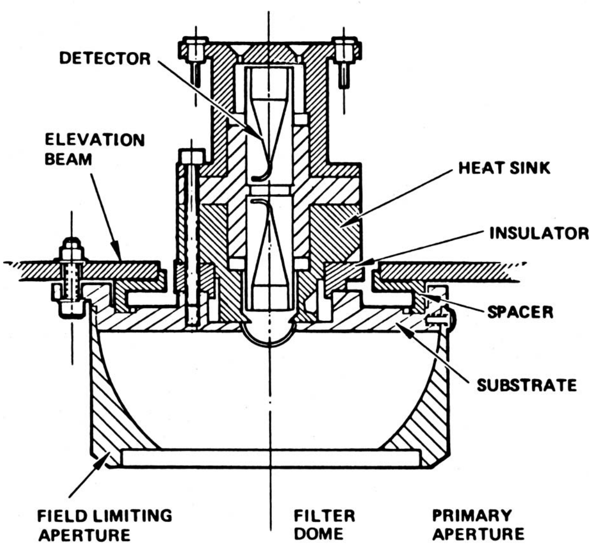

FIG. 4. Nonscanner sensor module. A shortwave channel sensor module schematic is shown, including the active and reference cones that detect the radiation, the filter dome, and the primary and secondary aperture limiters. The sensor modules are located in the elevation beam, which can be rotated to point the detectors at Earth, at the internal blackbodies, or at the solar ports.

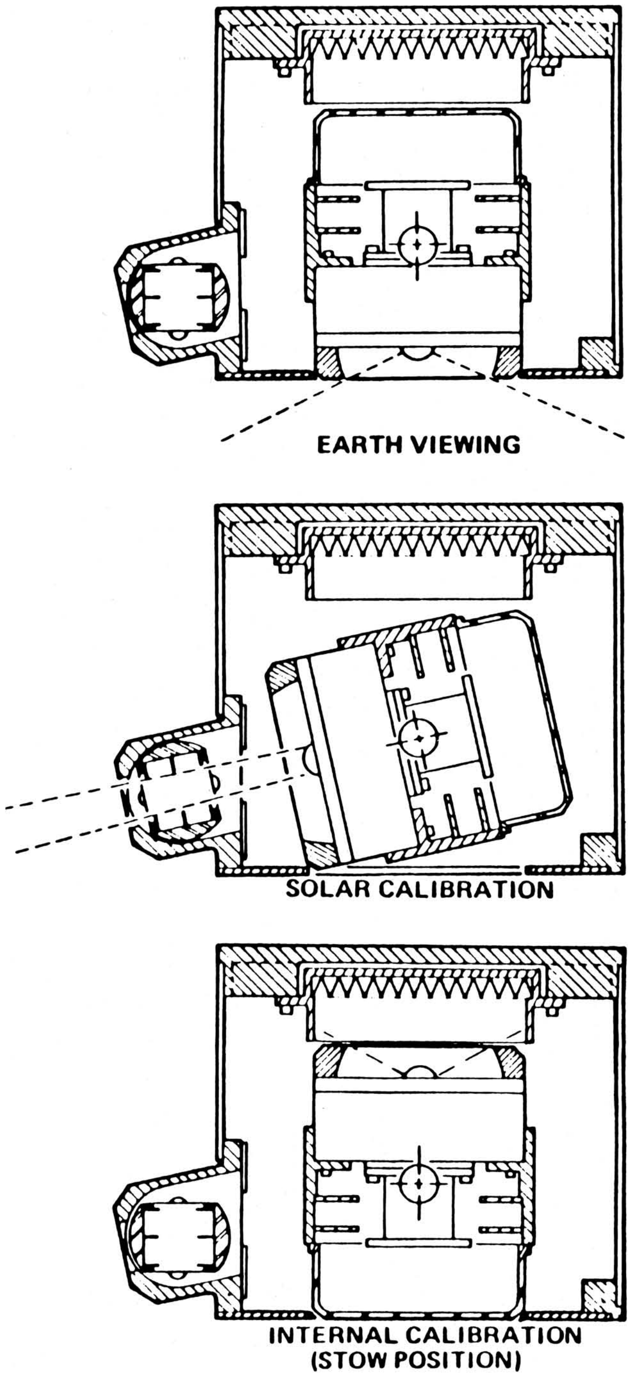

FIG. 5. Nonscanner elevation positions. The elevation beam in which the nonscanner detectors are mounted can be rotated to observe Earth, the Sun, or the internal blackbodies.

rotatable structure known as the elevation beam because it "elevates" the instruments to observe the Sun or the internal calibration sources, as shown in Fig. 5. The field-of-view limiters have been thermally connected with the elevation beam and decoupled from direct thermal flow through the detectors, so that temperature changes in these bodies will be small as well as monitored. The detector modules are actively controlled to operate at a higher temperature than the elevation beam in which they are mounted. The beam, in turn, is designed to operate at a higher temperature than the instrument head. Experience with the Engineering Model, a non-flying model with complete prototype detectors, has shown that the thermal controllers operate very stably, controlling the elevation–beam temperatures to better than $\pm$ 0.1 K. This eliminates a major source of instrument variability.

b. The scanner instruments

The ERBE scanner instrument package (see Fig. 3) contains three radiometric channels, each of which views the Earth, internal–calibration sources, and a solar–diffuser plate. The detectors are thermistors that use space on every scan as a reference point to guard against drift. They are located at the focal point of an f/1.84 Cassegrain telescope whose aluminum–coated mirrors have been overcoated to enhance ultraviolet reflectivity. Such a telescope has two mirrors: a large primary mirror and a smaller secondary one. Light is reflected from the primary to the secondary and is finally focused behind a hole in the primary. One of the channels has no filter, and so absorbs all wavelengths. A second has a fused-silica filter which transmits only shortwave radiation. The third has a multilayer filter on a diamond substrate to reject shortwave energy and accept longwave. To enhance the spectral flatness of the detectors, each thermistor chip is coated with a thin layer of black paint.

The instantaneous field of view of each channel is hexagonal, with an angular size of 3° by 4.5°, the longer dimension being along the satellite groundtrack. The hexagonal shape was derived through studies of aliasing in line-scanning electro-optical systems (Huck *et al.*, 1981).

The Nimbus 6 and 7 ERB instruments were designed with quite complex scanning patterns in order to maximize their ability to construct angular models of the reflected and emitted radiation (Smith *et al.*, 1977). The availability of angular models from this earlier mission (Taylor and Stowe, 1983) makes it possible for the ERBE scanner to scan only perpendicular to the orbit track. This pattern maximizes the spatial coverage of the detected pixels. In addition to crosstrack Earth scanning, the instrument head may be rotated about an axis through the nadir so that the Sun may be observed in reflection off the Mirror Attenuator Mosaic (MAM), a diffuser plate.

3. The ERBE calibration system

Fundamental to the design of the Earth Radiation Budget Experiment has been a requirement to be able to tie the radiation budget measurements directly to both the IPTS68 and to the World Radiometer Reference (WRR). This will be achieved through the use of a state-of-the-art ground-calibration facility, coupled with a complete inflight calibration system. The ground facility contains a Master Reference Blackbody (MRBB), an integrating sphere, and a reference solar monitor, as well as windows through which a solar simulator may be directed at the appropriate instrument. The in-orbit calibration will be maintained through the use of onboard blackbodies, an independently monitored incandescent lamp, and views of the Sun.

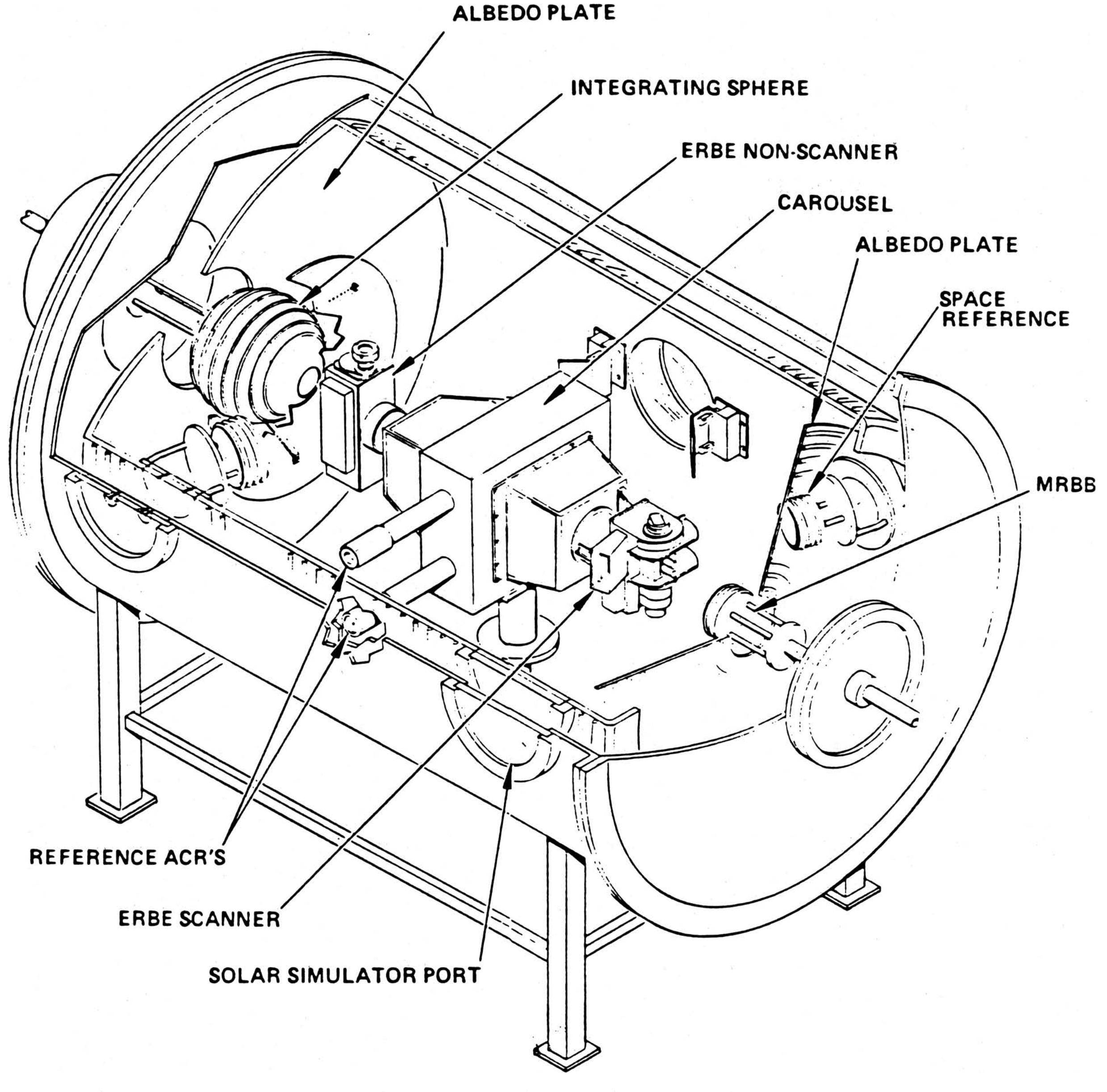

FIG. 6. ERBE calibration chamber. The ERBE calibration chamber is an 8-foot diameter cylinder containing a Master Reference Blackbody (MRBB) in the right door and an integrating sphere in the left door. The solar simulator can project a beam through a quartz window onto an instrument mounted on a carousel in the center of the chamber. Each end of the chamber has a liquid nitrogen cooled space reference source to allow space clamp of the ERBE scanner.

a. The ERBE ground calibration system

In the TRW plant where the ERBE instruments have been assembled, there is a complete calibration environment that was constructed specifically for ERBE. This environment, shown in Fig. 6, consists of a large thermal vacuum chamber whose walls can be chilled with liquid nitrogen (LN_2) and which contains both shortwave and longwave calibration sources. At one end of the chamber is a Master Reference Blackbody (MRBB) and associated equipment; at the other end, an integrating sphere. In addition to the cold shroud, the walls of the chamber contain a space source to provide the equivalent of a space look for scanner calibration and quartz windows through which light from the solar simulator may illuminate the instruments. In the center of the chamber, there is a carousel on which the ERBE instruments may be mounted.

b. The master reference blackbody

The fundamental tie to the IPTS68 is provided by the ERBE Master Reference Blackbody, illustrated in Fig. 7. This is a concentrically grooved piece of aluminum whose grooved surface is black anodized and in the back of which are mounted six platinum resistance thermometers (PRTs). To provide temperature stability, the aluminum is located in a thermally controlled housing. On the side visible to the instrument, there is a gold cone which assures that the instru-

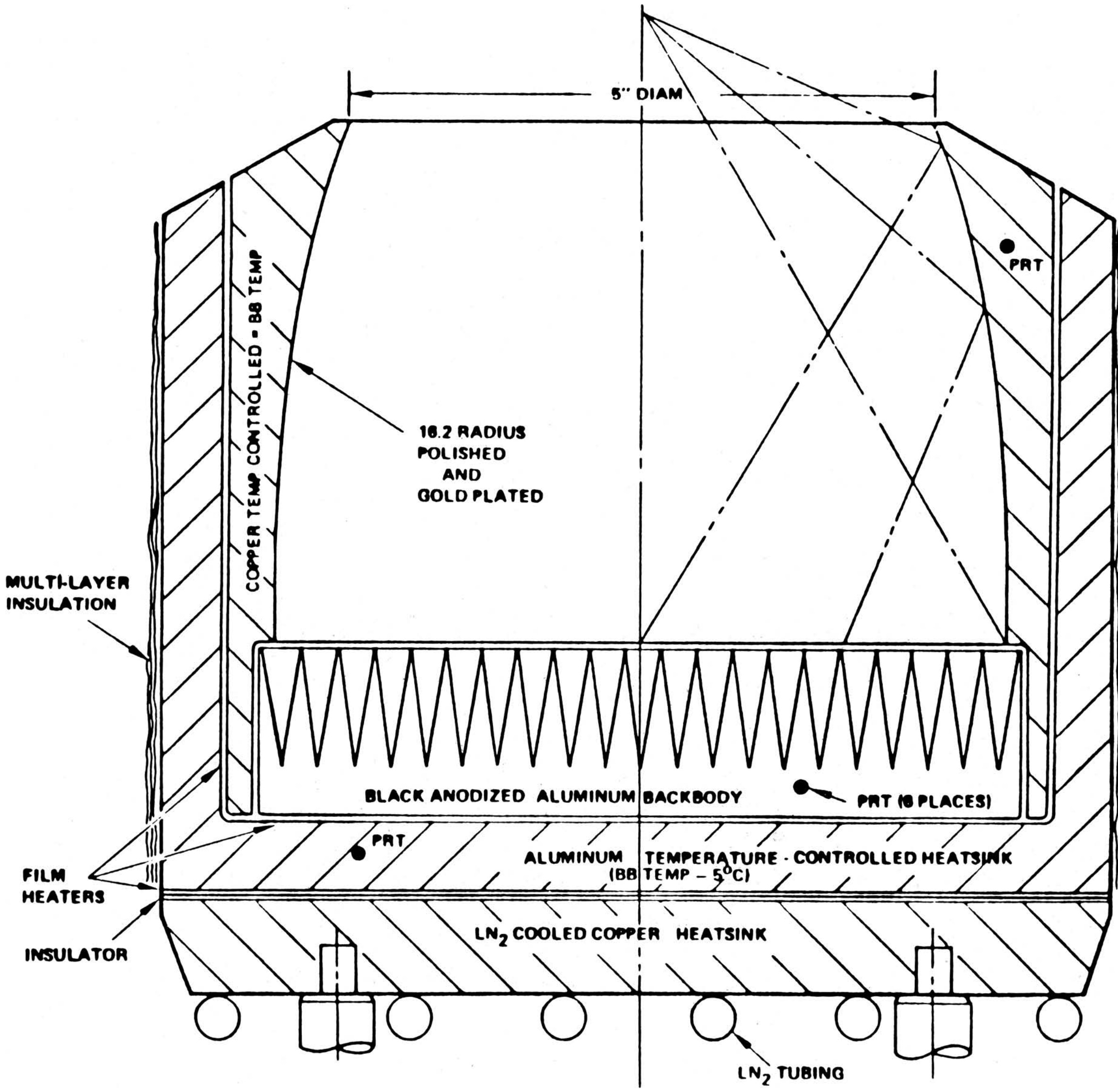

FIG. 7. Master Reference Blackbody (MRBB) cross–section. The primary radiometric reference for ERBE is provided by the Master Reference Blackbody. The radiating surface is a grooved piece of Aluminum with a black anodized face. The temperature traceability is provided by six calibrated Platinum Resistance Thermometers.

ment fields of view are completely filled by the blackbody. At the narrow end of the cone, where an instrument is placed during calibration, there is a grooved ring which is cooled to liquid nitrogen temperatures to simulate the energy exchange to space that occurs in flight operation of the instruments.

As a result of the care in construction and thermal engineering, the ERBE MRBB has proven to be capable of state–of–the–art accuracy. The absorptivity of the grooved surface has been measured at the Naval Ocean Systems Center as being 0.991. The temperature uniformity of the surface has been checked by observing the emitted radiation with a narrow field of view, infrared radiometer that moved just above the grooved surface. The spatial temperature variations appear to be less than $\pm$ 0.01 K over the operating range of the MRBB (-80°C to +75°C). The thermal control is accurate to $\pm$ 0.1 K over this temperature range.

c. The ERBE integrating sphere

The shortwave calibration of the ERBE instruments is provided by an integrating sphere, as shown in Fig. 8. The 20–inch diameter sphere has two different paint coatings and is illuminated by four 250–W tungsten lamps near its mouth. The lamps are part of a projection optics system that reflects the light off a mirror and then transmits it to the interior of the sphere through a piece of flashed opal glass. The layers of glass through which the light passes before entering the sphere serve to limit the admitted infrared radiation.

Its interior surface has two coats of paint: an undercoat of 3M White Velvet which adheres well to the surface of the sphere, and an overcoat of barium sulfate. When checked with a narrow field radiometer, the sphere's interior coat gives a uniform angular radiance to within a few percent. The stability of the shortwave radiation from the sphere is moni-

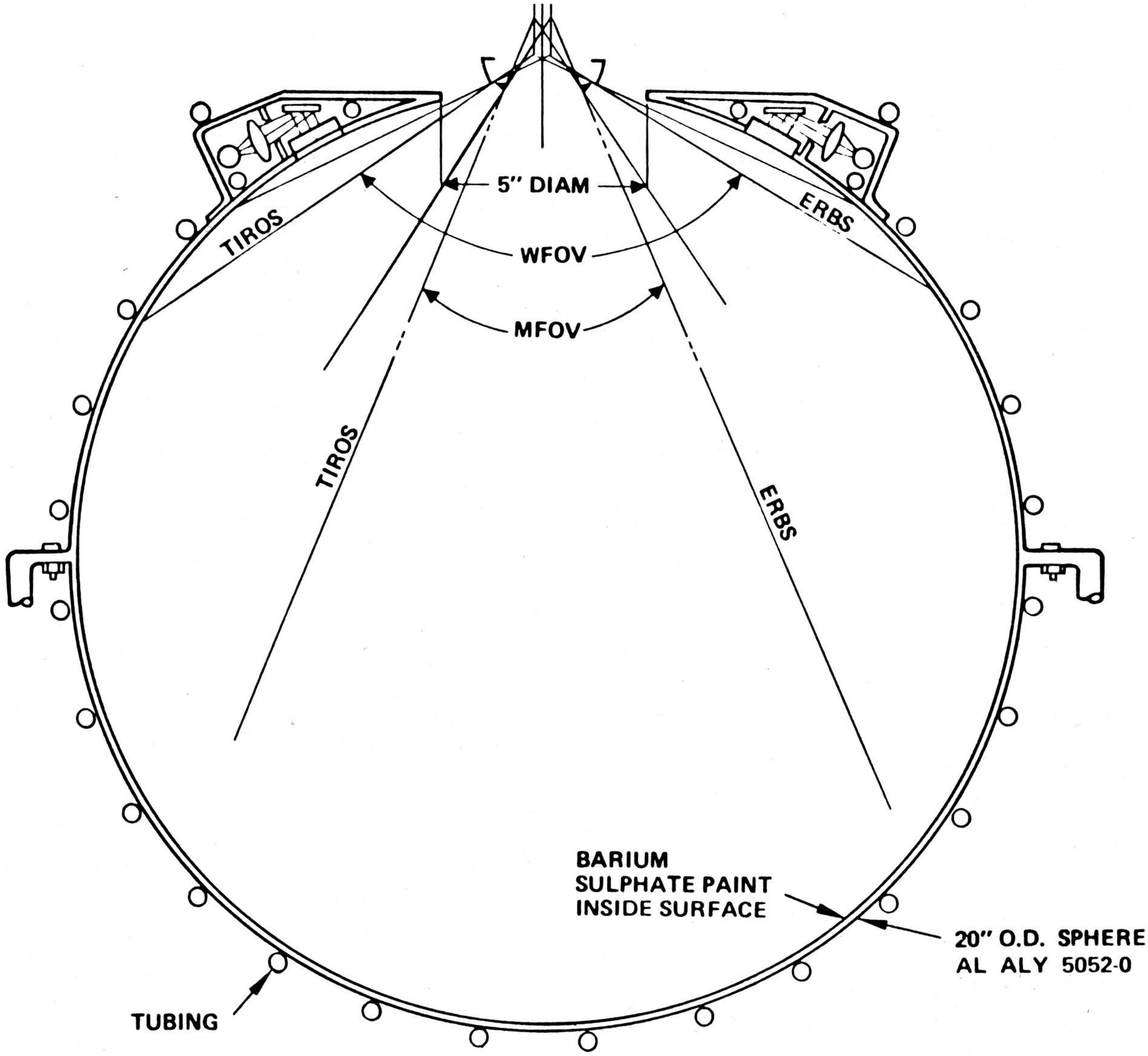

FIG. 8. Integrating sphere. Shortwave calibration is provided by an integrating sphere. The light is provided by four 250–W Tungsten bulbs that illuminate the sphere walls through projection optics near the mouth of the sphere.

tored with silicon photodiodes located near its mouth. To assure that the background infrared radiation from the sphere is reasonably stable, the sphere is thermally controlled by a flow of alcohol and water in a pipe wound around its outside.

d. The ERBE inflight calibration capability

All seven of the Earth–viewing channels on ERBE have inflight calibration capability. The total channels and the longwave scanner channel view blackbodies. Both the shortwave and total channels can view the Sun, and the former also views an internal incandescent source which is monitored by silicon photodiodes.

In stowed position, the nonscanner channels look up into the faces of blackbodies, as is illustrated in Fig. 5. These inflight calibration sources are similar to the Master Reference Blackbody, each being a piece of aluminum in which deep, concentric grooves have been cut. The grooved side of the blackbodies is anodized, while on the back there are heaters. In the center of the back, each blackbody has an individually calibrated platinum resistance thermometer.

For the shortwave channels, there is an internal calibration source whose light comes from an evacuated tungsten light bulb. The light is carried from the bulb to the entrance aperture of the detectors by fiber optics. At this point, it is monitored by a silicon photodiode, mounted so that its temperature may also be monitored. Due to the spectral dependence of the light, these sources do not form an absolute calibration standard. However, the lamps are stable at levels approaching one percent. Thus, any change in the instrument response from that in the ground calibration may be noted, and more detailed calibration checks with solar observations may be done immediately.

e. Solar observations

In both instrument packages, observations of the Sun may be made by commanding the spacecraft. With the nonscanner

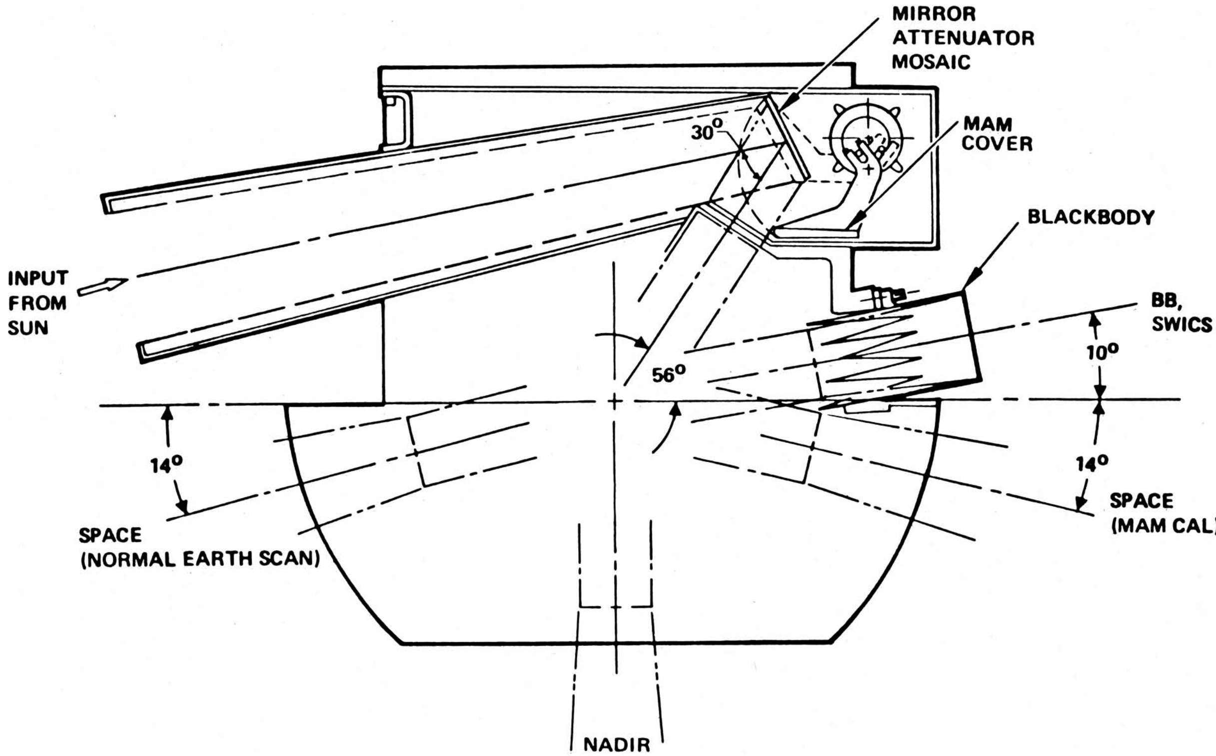

FIG. 9. Scanner inflight calibration geometry. The scanner can be calibrated in flight through an internal blackbody, or a tungsten filament lamp, as well as by observations of the Sun reflected from a diffuser plate known as a Mirror Attenuator Mosaic (MAM). For reference, the Earth is at nadir during these observations, and the detector is referenced by an observation of space every scan.

package, the instruments will move from their normal orientation to one in which the Sun drifts through the solar monitor field of view. This involves only a change in the instrument azimuth. The solar monitor will then be commanded to repeatedly cycle its shutter open for 32 seconds and closed for 32 seconds. In addition, the Earth-viewing channels can be rotated in elevation until they view the Sun through ports in the side of the instrument package. These ports are attached to the thermally controlled instrument body and their temperatures are monitored, so that changes in background infrared radiation can be taken into account.

For scanner solar calibration, the Sun's light is reflected from a diffuser, known as a Mirror Attenuator Mosaic (MAM). This is a small plastic plate that contains an array of nickel plated, hemispherical indentations. The MAM reflects isotropically over the range of viewing angles (the effect is very much like the reflection from an array of ball bearings or spherical mirrors). To prevent the multiple reflections that would occur if rays struck the balls too obliquely, the indentations are covered by a mask of blackened copper. This mask is thermally connected to the baffling system so that the MAM remains stable in temperature. During the initial calibration of the ERBE Engineering Model, observations showed that there was no thermal contamination of the shortwave channel. As with the nonscanner, the scanner observes its calibration sources by rotating to a calibration position, illustrated in Fig. 9.

f. The instrument analytical models

In a very simple view, the ERBE instruments are thermometers. Thus, they are extremely sensitive to heat flows. To the extent that this flow can be predicted from the design, the instrument data may be reliably interpreted; to the extent that it is unpredictable, interpretation is in question.

A more formal way of demonstrating the necessity for an explicit, analytical model of instrument operation is to consider an instrument as a function that maps incident radiation and internal heat flows into a sequence of integers on magnetic tape. The conversion of these integers, or counts, into radiances or radiant incidences is a second function. To the extent that the latter function is not an inverse of the former, the instrument and the data processing system are in error. Accordingly, every algorithm for converting instrument data to radiation contains a "ghost instrument" that is the inverse of the count conversion algorithm. Only to the extent that this "ghost" mirrors the actual hardware can the measurement of the satellite altitude radiation fields be regarded as correct.

Because of the importance of correctly describing the instrument behavior, the construction of instrument mathematical models has been part of the ERBE since its inception. The heat flow in thermal instruments, like those in ERBE, can be described by a system of linear equations in which the temperatures of the individual nodes are a vector of unknowns to be determined. A schematic of such a description is given in Fig. 10. The vector of nodal temperatures is multiplied by a matrix containing the thermal resistances and capacitances. The power input to the system appears on the righthand side of the equations. The solution of these equations relates the nodal temperatures to the sources of heat, including the radiation absorbed by the detector. The instrument electronics converts the temperature variations

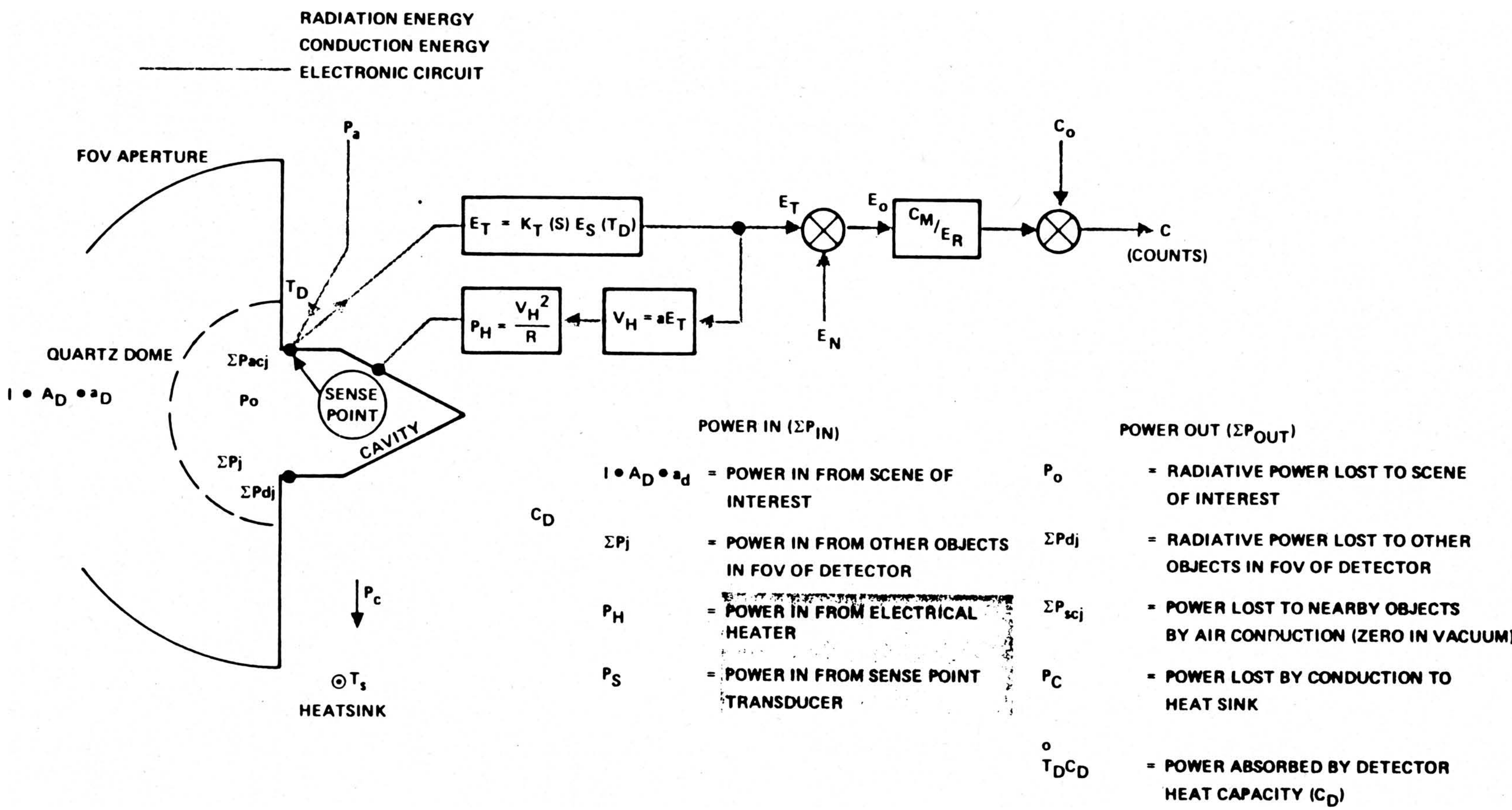

FIG. 10. Nonscanner thermal model schematic. A schematic of the thermal nodes for one of the nonscanner channels is shown. Radiation impinges on the detector from the left, whereby the cavity can exchange energy with the field-of-view (FOV) aperture and the heat sink. Electrical power is supplied to keep the cavity temperature constant. Various energy exchanges are shown in the details of this figure.

into variations in voltages that are telemetered to the ground. This is modeled by an electronic transfer function. The result is a rigorous count conversion algorithm, relating incident radiation to the telemetered counts in a way that is directly derivable from the physics of the detectors.

In addition to being used directly in the derivation of the count conversion algorithms, such an approach to predicting the behavior of the instruments also assists in choosing design parameters. The shape of the cavities and the choice of the surface finishes of the field-of-view limiters of the nonscanner detectors were governed by ray tracing studies of energy deposition. The size of the fused-silica filter domes was chosen on the basis of modeling work completed before ERBE was formally approved (Cooper and Luther, 1980).

4. Inversion of radiation from satellite altitude to the top of the atmosphere

Once the data sent to the ground have been converted to satellite altitude radiances, it must be brought to the top of the atmosphere before it can be useful to the meteorological community. In addition, the data being sought by the ERBE are not radiances, L, which emerge from the top of the atmosphere in a particular direction, but the radiant fluxes or exitances, M, which describe the energy loss per unit area. The two quantities may be related through an angular distribution function, R, also known as the bidirectional model (or bidirectional reflectance function in the case of the shortwave radiation), according to the equation

$$M \equiv \iint \mathrm{d}\,\phi' \mathrm{d}\,\theta'\, sin\,\theta'\, cos\,\theta'\, L(\theta',\phi') = \pi\, L/R. \quad (1)$$

In this equation, θ' is the zenith angle, and ϕ' the azimuthal angle used to describe the direction in which the radiation is propagating.

The relation between the satellite measurement and either L or M is more complicated than it may appear from Eq. 1. In all cases, the satellite radiometer integrates the radiance over the angles within the field of view. Thus, we can write

$$m = \iint \mathrm{d}\lambda\ \mathrm{d}\Omega\ SL, \quad (2)$$

where m is the "measurement," S is the angular and spectral sensitivity of the instrument, and L is the radiance at the entrance aperture of the radiometer. The integration is taken over the instrument field of view. By using the geometric relationships between the satellite position and the top of the atmosphere, as well as the angles making up the field of view, it is possible to rewrite the measurement Eq. 2 in the form of a Fredholm integral equation of the first kind in two variables, relating m to the desired quantity, M:

$$m = \int \mathrm{d}A\ G\ S\ (R/\pi)M. \quad (3)$$

In this equation, $\mathrm{d}A$ is an element of area on the top of the atmosphere from which radiation emerges at angles θ' and ϕ'. We can then write the factor

$$G = (cos\,\theta'\, cos\,\zeta\,) \cdot \rho^{-2}, \quad (4)$$

where ζ is the nadir angle at which radiation strikes the detector, and ρ is the distance from the radiating area $\mathrm{d}A$ to the detector.

In the case of the scanner measurements, it is generally assumed that the radiation field can be regarded as homogeneous over the field of view of the instrument. With this assumption, it is possible to reduce the measurement equation to essentially Eq. 1. The major difficulty in inverting the data to the top of the atmosphere is the choice of bidirectional function. The first step is to use the three spectral channels to deduce spectrally flat longwave and shortwave radiances. With longwave and shortwave available, it is possible to cluster the observations into clear or cloudy scenes. Very roughly, we expect clear scenes to be dark and hot, cloudy to be bright and cold. The bidirectional functions themselves are based primarily on the ERB data from Nimbus 7 (Taylor and Stowe, 1983) although other data sources will be blended in, including models derived from GOES and AVHRR data.

In the case of the nonscanner, the observations cannot be reduced to the homogeneous field-of-view problem, and the full Eq. 3 must be solved. This problem is mathematically equivalent to the standard profile inversion problem in remote sounding. The basic technique is to represent the function M in terms of a set of basis functions, such as constant strips perpendicular to the subsatellite track, so that the integral can be represented as a sum. A sequence of observations then becomes a system of linear equations. In matrix form, the observations appear on the right-hand side, and the desired radiant exitance appears as a vector multiplied by a matrix. The matrix is typically ill-conditioned, so that care must be taken in the solution of the equations. With this care, the desired radiant exitance can be written as a suitably weighted sum of the observations along the satellite groundtrack. The mathematical formulation of the nonscanner inversion problem, as well as the development of various solution techniques, are described in several places, including House and Jafolla, 1980; Smith and Green, 1981; Bess *et al.*, 1981; Green, 1983; and King and Curran, 1980.

5. Averaging measurements over time and space

The process of measuring the radiation budget with satellite instruments and reducing it to the top of the atmosphere does not complete the work that must be performed. The radiation budget acts on the atmosphere and oceans over periods that are believed to be on the order of a week or longer, and over spatial scales that are a few hundred km or larger. Accordingly, the data reduction process must average the data to spatial resolutions of 250 km and larger, as well as averaging over time.

There are two types of variabilities that must be taken into account in averaging over time. The first is the "systematic" variation of albedo with solar-zenith angle, even for homogeneous surfaces. The second variation is that associated with variations in meteorology, most importantly changes in cloudiness, but also including the variation in emitted-longwave radiation associated with surface heating and cooling.

Because satellites do not remain fixed over a given geographic region unless they are in a geostationary orbit, observations from the normal meteorological satellites or the inclined orbit of the ERBS satellite require interpolation in

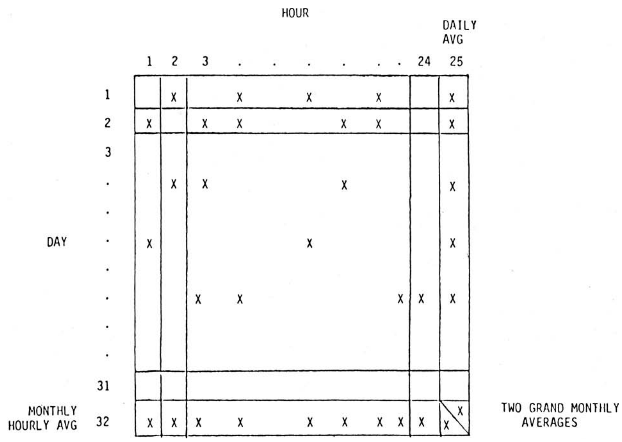

FIG. 11. Hourly–monthly array for temporal averaging. For ERBE data reduction, the Earth is divided into 10 368 2.5° regions. For each region, one month's observations are sorted into a time series arranged as shown in this figure. A month is divided into the appropriate number of days, each consisting of 24 hours. Within each hour–month box, all data at a given spatial resolution are averaged together to produce a single estimate at the center of the hour.

time. The basic data structure that is used in this part of the ERBE data processing is an hourly–monthly array, as shown in Fig. 11. The hours in a month can be formed into rows of 24 hours and placed in successive rows with one day under the other. If there were a satellite that could observe all hours in a month, daily averages could be formed simply by adding the radiation for each box in a row and dividing by 24. The average radiation at the end of a month could then be produced by adding the right-hand column and dividing by the number of rows.

For ERBE, as in previous satellite radiation budget missions, the expected satellite complement will leave some hours unsampled in most regions. The three satellites have been chosen so that they will cover as many of the hourly monthly boxes as possible within budgetary and launch constraints. It should be clear that Sun-synchronous orbits provide a sampling in which given times of day are observed only at a particular latitude, as shown in Fig. 12a. For example, a noon Equator-crossing satellite never sees the equatorial regions at 9:00 a.m. or 3:00 p.m. local solar time, and does not see regions with latitudes greater than 45°N at noon or midnight. A satellite without a Sun-synchronous orbit has a precessing orbital plane. For the ERBS orbit, at an altitude of 600 km and an inclination of 57°, the celestial longitude of the ascending node precesses about 4.95° west per day. Thus, over the course of 36 days, the orbit will rotate through about 180°, and the satellite will observe a much larger sample of hourly–monthly bins, as shown in Fig. 12b. The ERBE system of satellite observations has been chosen to provide an optimum set of observations (Harrison *et al.*, 1983, from which the last two figures have been taken).

With the hourly–monthly data structure in mind, the time averaging portion of the ERBE data processing first sorts the inverted data into a list of observations that can be accessed by geographic region and time of observation. As the data emerge from the inversion portion of the processing system, each scanner estimate and each 32-second average nonscanner estimate are Earth-located within one of 10 368 geographic bins that are produced by a 2.5° grid in latitude and longitude.

For each region, the radiation field is then interpolated for missing values in each hour box. In the longwave, simple linear interpolation will be used in most cases. In the shortwave, a more complicated scheme is necessary because the variation of albedo with solar zenith angle is different for different surfaces. The inversion portion of the processing system has classified a geographic region into 1 of 13 different scene types for each scanner observation as part of the choice of angular, directional model. This classification also provides an estimate of albedo variation with solar-zenith angle for each scene type at the time of observation. The scene type is

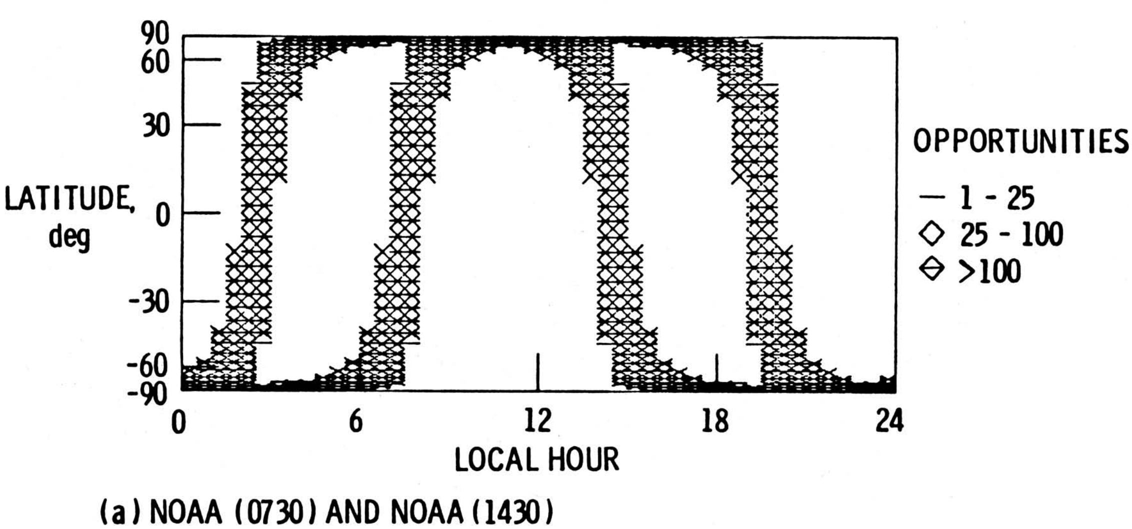

FIG. 12a. Temporal sampling as a function of latitude for a Sun-synchronous satellite. For a Sun-synchronous satellite, a given latitude is sampled in a regular pattern, as shown in this figure.

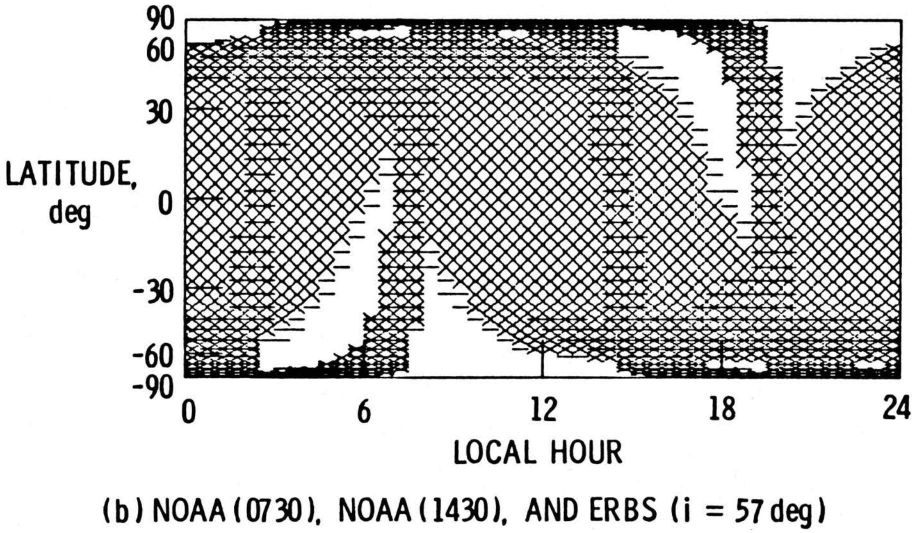

FIG. 12b. Three satellite sampling of time as a function of latitude for a month of observations. For ERBE, with a Sun–synchronous satellite and an inclined orbit satellite, temporal coverage over one month is much improved over the sampling with a single Sun–synchronous satellite alone.

assumed to vary linearly between observations, and the time variation of reflected radiation is constructed:

$$M(t) = \sum_{\substack{i\,=\,\text{scene}\\ \text{type}}} a_i(\mu_0\,(t_i))\;\delta_i(\mu_0(t))\;E_0\;\mu_0\,(t). \tag{5}$$

In this equation, a_i is the observed albedo at the time of observation for a given scene type, δ_i is the albedo variation with solar zenith angle of that scene type normalized to overhead Sun, μ_0 is cosine of solar zenith, and E_0 is the solar irradiance at the time of observation. The integration over time is approximated by using discrete values for a given hour and adding up the contributions from different hours.

The averaging process will be performed for each of the 10 368 regions for each month of data processed. The hourly-monthly boxes will also be used to combine the observations by various satellites and various resolutions that are produced by the ERBE ground processing system.

6. Organizational considerations

NASA Headquarters, through the Earth Science and Applications Division of the Office of Space Science and Applications, oversees the ERBE Project. Goddard Space Flight Center is responsible for the ERBS spacecraft. Langley Research Center (LaRC) is responsible for instrument procurement and development and operational data processing, as well as operations of the ERBE Science Team. Expected launch information is given in Table 3.

The success of ERBE depends critically upon the ground-processing software. Accordingly, this software has been developed in a way that should minimize errors and make the system modular, so that only small portions of the system are affected by individual errors. The system has been developed in three releases. Each release began with specifications from the ERBE Science Team, and was followed by detailed design, coding and testing. This process has provided a chance to rewrite the software as mistakes and misunderstandings have been found. It also has allowed the software to be "group property," decreasing the reliance on one individual and thereby decreasing the number of errors.

After launch, the Science Team, together with members of Langley Research Center concerned with the instruments, will validate the ERBE data products. The Science Team members will also participate in initial data use investigations with the ERBE data. The team was selected in November 1979 to provide a balance of expertise in the following areas:

1) Instrument thermal and radiometric modeling and calibration;

TABLE 3. ERBE launch information.

Platform	Orbital Altitude (km)	Orbital Inclination (deg)	Equatorial Crossing Local Solar Time (h)	Earliest Expected Launch Date
ERBS	600	57	—	October 1984
NOAA F	833	98 (Sun Synch)	0730	November 1984
NOAA G	833	98 (Sun Synch)	1530	August 1985

2) Algorithm development for inversion of ERBE data to the top of the atmosphere and for averaging over time and space; and

3) Scientific knowledge of the physical processes of the atmosphere and the associated use of data in determining the Earth's radiation budget and its relation to other atmospheric processes.

The team has organized itself into four working groups, according to the detailed breakdown of the work that has been discussed previously. These working groups are Instrument (Ins.), Inversion (Inv.), Averaging (TSA), and Data Products (DP). The Science Team and membership in working groups are given in Table 4.

TABLE 4. ERBE science team information.

Principal Investigator	Working Group	Institution	Co-Investigators	Description of Investigations
B. Barkstrom[a]		NASA LaRC	D. Crommelynck M. Luther L. Kopia	Instrument thermal modeling and radiation budget statistical studies
A. Berroir	DP	Laboratoire de Meteorologie Dynamique, France	R. Sodorny K. Laval A. Chedin N. Scott Y. Fouquart J. Morcrette	Improvement of radiation modelization in a general circulation model
R. Cess[c]	Instr.	State Univ. of New York—Stony Brook		Validation of models predicting radiation budget variations and investigate climatic feedback effects
C. Duncan	Instr.	Consultant		Calibration and evaluation of ERBE sensors
A. Gruber	DP, TSA	NOAA-NESS	H. Jacobowitz L. Stowe P. Abel I. Ruff P. Rao T. Chen J. Wydick	Develop angular models and inter compare ERBE data with atmospheric constituents and operational satellite measurements
E. Harrison[c]	TSA	NASA LaRC	D. Brooks P. Minnis	Diurnal variation of cloudiness and radiation budget
D. Hartmann	TSA	University of Washington	J. Wallace	Diurnal cycle of radiation budget and effects of cloudiness on net radiation
F. House	Inv.	Drexel Univ.		Application of optimal estimation techniques to data use investigation
F. Huck	Instr.	NASA LaRC	N. Halyo S. Park W. Staylor S. Choi	Assessment of sensor performance and measurement accuracy
G. Hunt[c]	DP	Imperial Coll. London, England	B. Hoskins C. England	Regional radiation budgets compared to those from geostationary data and use SAGE II data to understand effects of other atmospheric constituents
R. Kandel	TSA	Centre National de la Recherche Scientifique, France		Diurnal variation and the Earth radiation measurements
J. Kibler	DP	NASA LaRC (Ex Officio)		Operational ERBE Processing System
M. King[b]	Inv.	NASA GSFC	R. Davies	Effect of clouds on satellite albedo measurements

TABLE 4. (*Continued*)

Principal Investigator	Working Group	Institution	Co-Investigators	Description of Investigations
A. Miller	DP	NOAA–NMC	A. Krueger	Dynamical interpretation of ERBE information
A. Mecherikunnel	Ins.	NASA GSFC	J. Gatlin B. Guenther	Sensor performance in space and solar data analysis
V. Ramanathan	DP, Inv.	NCAR	J. Coakley P. Downey B. Briegleb D. Baldwin	Using ERBE measurements to validate and improve radiation models and general circulation climate models
E. Raschke	Inv.	University of Cologne, FRG	P. Speth E. Ruprecht R. Stuhlmann M. Wiegner	Investigate surface and regional radiation budgets and improve model parametrizations
L. Smith[c]	Inv.	NASA LaRC	L. Avis T. Bess R. Green J. Suttles B. Wielicki	Algorithm development and investigation of radiation budget variability
W. Smith	TSA, Instr.	University of Wisconsin	V. Suomi L. Sromovsky H. Revercomb F. Nagle	Investigate time/space lags of radiation budget compared to other meteorological variability
T. Vonder Haar	TSA	Colorado State University	G. Campbell E. Smith	Algorithm development for averaging ERBE data over time and space and synergistic investigations with SAGE II data

[a] ERBE experiment scientist and Science Team leader. [b] GSFC ERBE project scientist. [c] Working group leader.

Acknowledgments. This article would have been impossible without the contributions of a very large number of individuals. Members of the ERBE Science Team have been invaluable in this regard. Indeed, the authorship might reasonably be considered to belong to the Science Team as a whole. In addition, J. E. Cooper, ERBE experiment manager; M. Luther and L. Kopia, ERBE instrument engineers; and S. Carmen and R. Hesser of TRW have played crucial roles in the design of the ERBE instruments and the TRW calibration facility.

References

Bess, T. D., R. N. Green, and G. L. Smith, 1981: Deconvolution of wide-field-of-view radiometer measurements of Earth-emitted radiation. Part II: analysis of first year of Nimbus 6 ERB data. *J. Atmos. Sci.*, **38,** 474–488.

Bignell, K. J., 1961: Heat balance measurements from an Earth satellite: an analysis of some possibilities. *Quart. J. Roy. Meteor. Soc.*, **87,** 231–244.

Cess, R. D., 1976: Climate change: an appraisal of atmospheric feedback mechanisms employing zonal climatology. *J. Atmos. Sci.*, **33,** 1831–1843.

Cess, R. D., B. P. Briegleb, and M. S. Lian, 1982: Low-latitude cloudiness and climate feedback: comparative estimates from satellite data. *J. Atmos. Sci.*, **39,** 53–59.

Cooper, J. E. and M. R. Luther, 1980: Performance of fused silica as a filter in a wide-field-of-view Earth radiation budget radiometer. *Appl. Opt.*, **19,** 1798.

Ellis, J. S., T. H. Vonder Haar, S. Levitus, and A. H. Oort, 1978: The annual variation in the global heat balance of the Earth. *J. Geophys. Res.*, **83,** 1958–1962.

Green, R. N., 1983: Accuracy and resolution of Earth radiation budget estimates. *J. Atmos. Sci.*, **40,** 977–985.

Harrison, E. F., P. Minnis, and G. G. Gibson, 1983: Orbital and cloud cover sampling analyses for multisatellite Earth radiation budget experiments. *J. Spacecraft and Rockets,* **20,** 491–495.

Hartmann, D. L., and D. A. Short, 1980: On the use of Earth radiation budget statistics for studies of clouds and climate. *J. Atmos. Sci.*, **37,** 1233–1250.

House, F. B., and J. C. Jafolla, 1980: One-dimensional technique for enhancing Earth radiation budget observations from Nimbus 7 satellite. *Proc. International Rad. Symp.*, Fort Collins, Colorado.

Huck, F. O., N. Haylo, and S. K. Park, 1981: Information efficiency of line-scan imaging mechanisms. *Appl. Opt.*, **20,** 1990–2007.

King, M. D., and R. J. Curran, 1980: The effect of a nonuniform planetary albedo on the interpretation of Earth radiation budget observations. *J. Atmos. Sci.*, **37,** 1262–1278.

Lorenz, E. N., 1967: *The Nature and Theory of the General Circulation of the Atmosphere,* WMO, Geneva.

Ohring, G., and P. Clapp, 1980: The effect of changes in cloud amount on the net radiation at the top of the atmosphere. *J. Atmos. Sci.*, **37,** 447–454.

Oort, A. H. and T. H. Vonder Haar, 1976: On the observed annual cycles in the ocean–atmosphere heat balance over the northern hemisphere. *J. Phys. Oceanogr.*, **6,** 781–800.

Ramanathan, V., 1977: Interactions between ice-albedo, lapse-rate and cloud-top feedbacks: an analysis of the nonlinear response of a GCM climate model. *J. Atmos. Sci.*, **34**, 1885–1897.
Raschke, E., T. H. Vonder Haar, W. R. Bandeen, and M. Pasternak, 1973: The annual radiation balance of the Earth atmosphere system during 1969–70 from Nimbus 3 measurements. *J. Atmos. Sci.*, **30**, 341–364.
Schneider, S. H., and R. E. Dickinson, 1974: Climate modeling. *Rev. Geophys. Space Phys.*, **12**, 447–493.
Slingo, J. M., 1982: A study of the Earth's radiation budget using a general circulation model. *Quart. J. Roy. Meteor. Soc.*, **108**, 379–405.
Smith, G. L., and R. N. Green, 1981: Deconvolution of wide-field-of-view radiometer measurements of Earth-emitted radiation. Part I: theory. *J. Atmos. Sci.*, **38**, 461–473.
Smith, W. L., H. B. Howell, H. Jacobowitz, D. T. Hillery, J. Hickey, and A. J. Drummond, 1977: Nimbus 6 Earth radiation budget experiment. *Appl. Opt.*, **16**, 306–318.
Stephens, G. L., G. C. Campbell, and T. H. Vonder Haar, 1981: Earth radiation budgets. *J. Geophys. Res.*, **86**, 9739–9760.
Suomi, V. E., 1958: The radiation balance of the Earth from a satellite. *Annals of the IGY*, **1**, 331–340.
Taylor, V. R., and L. L. Stowe, 1983: Reflectance characteristics of uniform Earth and cloud surfaces derived from Nimbus 7 ERB. Submitted to *J. Geophys. Res*, **89**, 4987–4996.
Vonder Haar, T. H., 1969: Meteorological applications of reflected radiance measurements from ATS 1 and ATS 3. *J. Geophys. Res.*, **7**, 5404–5412.
——, 1970: Application of simultaneous infrared radiation measurements and cloud photographs from satellites. *J. Appl. Meteor.*, **9**, 955–958.
——, and V. E. Suomi, 1969: Satellite observations of the Earth's radiation budget. *Science*, **163**, 667–669.
Willson, R. C., S. Gulkis, M. Janssen, H. S. Hudson, and G. A. Chapman, 1981: Observations of solar irradiance variability. *Science*, **211**, 700–703. •

announcements[1]

International Fellowships for Women of Countries other than the United States

The American Association of University Women (AAUW) Educational Foundation awards international fellowships for advanced study and training to women of outstanding ability who are citizens of countries other than the United States. There are no restrictions as to the age of the applicant or the field of study. Upon return to their own countries, fellowship recipients are expected to provide effective leadership in their fields.

About 60 international fellowships are awarded yearly, for one year's graduate study or advanced research at an approved institution in the U.S. Women who are members of national associations in their own countries or of federations affiliated with the International Federation of University Women (IFUW) are eligible for six AAUW-IFUW awards, which are made for advanced research in any country other than the fellow's own. All awards are for one academic year, beginning in September, and are non-renewable. The amount of the award is $10,000.

For information on qualifications and limitations, or for an application form, write to AAUW Educational Foundation Programs, 2401 Virginia Avenue NW, Washington, DC 20037, U.S.A. Include the country of which you are a citizen. The application fee is $5.00 (U.S.).

[1]Notice of registration deadlines for meetings, workshops, and seminars, deadlines for submittal of abstracts or papers to be presented at meetings, and deadlines for grants, proposals, awards, nominations, and fellowships must be received at least three months before deadline dates.—*News Ed.*

Applications Sought for Senior and Postdoctoral Research Associateships

The National Research Council announces the 1985 postdoctoral, resident and cooperative research associateship programs for research in science and engineering to be conducted in behalf of 21 federal agencies and research institutions, located throughout the U.S. The programs provide Ph.D. scientists and engineers of unusual promise and ability with opportunities to do research on problems of their own choosing, yet compatible with the research interests of the supporting laboratory. Initiated in 1954, the associateship programs have contributed to the career development of over 4000 scientists.

Approximately 250 full-time associateships will be awarded on a competitive basis in 1985 for research in chemistry, engineering, and mathematics, and in earth, environmental, physical, space, and life sciences.

Awards are made for one or two years; senior applicants who have held the doctorate at least five years may request shorter tenures. Stipends for the 1985 year will begin at $25,350 for recent Ph.D.s and will be individually determined for senior associates. A stipend supplement up to $5,000 may be available to awardees holding recognized doctoral degrees in those disciplines where the number of degrees conferred by U.S. graduate schools is significantly below the current demand.

Information on specific research opportunities and federal laboratories, and application materials may be obtained from Associateship Programs, Office of Scientific and Engineering Personnel, JH 608-D3, National Research Council, 2101 Constitution Avenue NW, Washington, DC 20418, phone 202-334-2760. The application deadline is 15 January 1985.

(continued on page 1200)